MedChemComm

Synthesis of a new HYNIC-DAPI derivative for labelling with ^{99m}Technetium and its in vitro evaluation in an FRTL5 cell line

Journal:	*Medicinal Chemistry Communications*
Manuscript ID:	MD-CAR-12-2014-000574.R2
Article Type:	Concise Article
Date Submitted by the Author:	06-Mar-2015
Complete List of Authors:	Ferl, Sandra; TU Dresden, Faculty of Medicine Carl Gustav Carus, Department of Nuclear Medicine Wunderlich, Gerd; TU Dresden, Faculty of Medicine Carl Gustav Carus, Department of Nuclear Medicine Smits, René; ABX advanced chemical compounds, Hoepping, Alexander; ABX advanced chemical compounds, Naumann, Anne; TU Dresden, Faculty of Medicine Carl Gustav Carus, Department of Nuclear Medicine Kotzerke, Jörg; TU Dresden, Faculty of Medicine Carl Gustav Carus, Department of Nuclear Medicine

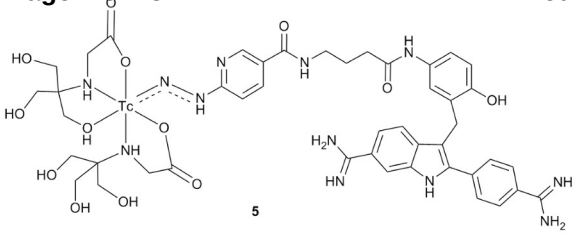

Supposed Strukture of the new 99mTc-(tricine)nHYNIC-DAPI derivative with HYNIC as monodentate ligand.

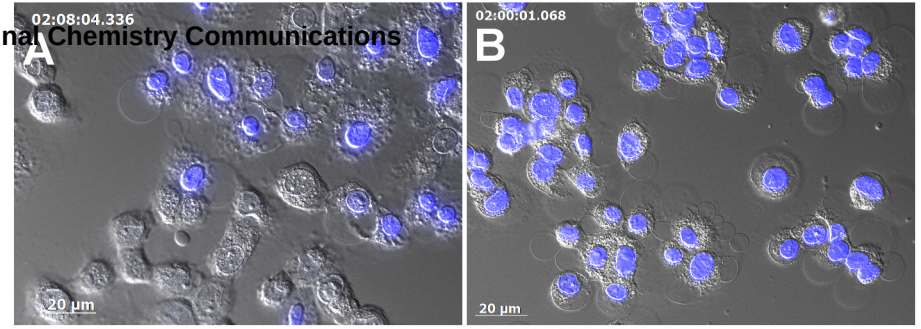

Distribution characteristics of unlabelled HYNIC-DAPI (A) in comparison to DAPI (B) in living FRTL5 cells. Live cell images with correlation of differential interference contrast (DIC) technique and DAPI filter (Axio Observer Z.1 microscope, Zeiss).

Synthesis of a new HYNIC-DAPI derivative for labelling with ^{99m}Technetium and its *in vitro* evaluation in an FRTL5 cell line†

Sandra Ferl,*[a] Gerd Wunderlich,[a‡] René Smits,[b] Alexander Hoepping,[b] Anne Naumann,[a] and Jörg Kotzerke[a]

Received Xth XXXXXXXXXX 20XX, Accepted Xth XXXXXXXXX 20XX
First published on the web Xth XXXXXXXXXX 200X
DOI: 10.1039/b000000x

4',6-diamidine-2-phenylindole (DAPI) is a common fluorochrome that is able to bind to deoxyribonucleic acid (DNA) with distinct, sequence depending enhancement of fluorescence. This work presents a possibility for the synthesis of a new multifunctional compound, that includes the fluorescent dye as a ^{99m}Technetium (^{99m}Tc) carrier. A new technique for the bioconjugation of DAPI with 6-hydrazinonicotinic acid (HYNIC) through an amide linkage was developed. The radiolabelling was performed with HYNIC as chelator and *N*-(2-hydroxy-1,1-bis(hydroxymethyl)ethyl)glycine (tricine) as coligand. Furthermore, experimental evidence showed that ^{99m}Tc complexes with DAPI as DNA-binding moieties are detectable in living fisher rat thyroid follicular cell line 5 (FRTL5) and their nuclei. The investigations indicated further, that the new HYNIC-DAPI derivative is able to interact with double-strand DNA. This establishes the possibility to locate ^{99m}Tc in close proximity to biological structures of living cells, of which especially the genetic information carrying cell compartments are in the centre of the interest. In this context, further investigations are related to the radiotoxic effects of DNA-bound ^{99m}Tc-HYNIC-DAPI derivatives and dosimetric calculations.

1 Introduction

Today's level of knowledge in medicine affords a number of therapeutic options against carcinosis. One important area of expertise is nuclear medicine, in which beta emitting radio nuclides are used for therapy, for instance, ^{131}I, ^{188}Re, ^{90}Y, or ^{177}Lu[1,2]. Recently, the radio metal ^{99m}Tc has become of interest. Because of its gamma radiation at 140 kilo electron volt (keV), it is commonly used for scintigraphy in nuclear medicine[3]. Furthermore, ^{99m}Tc emits an average of five Auger and internal conversion electrons per decay. Auger processes are able to damage DNA, depending on the proximity of the radionuclide to the genetic material[2,4,5]. This provides a possibility for radionuclide therapy with ^{99m}Tc that has already been demonstrated by several groups and is the subject of recent dosimetric investigations[6–9]. Various cell experiments showed that low-energy electrons located outside the cell nucleus are relatively non radiotoxic, whereas intranuclear decay proximate to DNA causes single- and double-strand breaks[10–13]. The difficulty in the use of Auger emitters in radionuclide therapy is that the radiotracer has to cross several physiological barriers and also has to be specific for the nucleus or DNA[14]. For this reason, the low accumulation rates of these radiotracers in living cells are the major limitation for therapeutic use. To take advantage of the potential of ^{99m}Tc as an Auger emitter, the development of multifunctional radio nuclide complexes, which accumulate in the cell nucleus, is necessary. They include a complexing agent for the radio nuclide as a carrier for the transport through different cell barriers into the nuclei of living cells and a DNA binding moiety. There are various studies in this field of science, for example, with oligonucleotides[15,16], antibodies[17], peptides[18], large molecules containing nuclei localisation sequences (NLS)[19], anthracenyl fragments[20,21], desoxyuridine[22], acridine derivatives[18], and Hoechst derivatives[23,24] as carrier for different Auger emitters. Based on these results we developed a new approach with DAPI, a commonly used fluorescent dye for staining cell nuclei, as a carrier for ^{99m}Tc. It was first synthesised by Dann et al. in the search for a new trypanocide and is an analogue of diary-

[a] *Technische Universität Dresden, Faculty of Medicine Carl Gustav Carus, Department of Nuclear Medicine, Fetscherstraße 74, 01307 Dresden, Germany; E-mail: Sandra.Ferl@gmx.de*
[b] *ABX advanced biochemical compounds GmbH, Heinrich-Gläser-Straße 10-14, 01454 Radeberg, Germany*
‡ Principal Corresponding Author; Email: Gerd.Wunderlich@uniklinikum-dresden.de
† Electronic Supplementary Information (ESI) available. See DOI: 10.1039/b000000x/

lamidine (berenyl)[25]. Although not enforced in medical application until now, DAPI is widely used for biological and cytochemical investigations[26–28]. Among its various biological effects including antibiotic, antitrypanosomal, and antiviral activity, it is characterised by the binding to DNA or ribonucleic acid (RNA)[29–31]. It was found that two distinct modes of interaction may occur, depending on the sequence of DNA: a selective coupling to the minor groove with adenine-thymine base pair (AT)-selective, distinct increase of fluorescence quantum yield and an intercalative binding to guanine-cytosine base pair (GC) with low fluorescence that is comparable to the free dye[28,32,33].

Our working group aims to develop a combination of the DNA binder DAPI with the radio nuclide ^{99m}Tc to investigate the biological effectiveness of the Auger emitter localised in the nuclei of living cells. Mainly, DAPI should act as a ^{99m}Tc carrier through different cell barriers, as a DNA binding moiety, and the fluorescence of the dye should enable optical visualisation of the multifunctional compound. Neither DAPI nor the new derivative were selective for a cell line or a special tumour tissue. The new radiotracer should act as a tool for the investigation of the damaging potential of an Auger emitter under *in vitro* conditions and should enable the acquisition of significant data for dosimetric calculations. To obtain a combination of the fluorescent dye with the radio nuclide, HYNIC was chosen as a chelator for ^{99m}Tc, which was coupled to DAPI through an amide linkage. The Technetium(V)-HYNIC system was firstly introduced by Schwartz et al.[34] and allows ^{99m}Tc labelling with very high specific activity under mild conditions. Furthermore, the convertibility of coligands provided the opportunity to influence the stability or the biodistribution of the ^{99m}Tc complex[35,36]. Because HYNIC occupies either one or two coordination sites of ^{99m}Tc, the coordination sphere must be completed by a coligand. The current investigations were made with tricine, one of the most commonly used coligands, whose complexing reaction with ^{99m}Tc is described as fast and efficient under mild conditions[37–43]. To prove the influence of the spacer between DAPI and HYNIC, different HYNIC-DAPI derivatives were synthesised that will be presented in forthcoming publications. This work describes the synthesis and characterisation of one derivative with a spacer based on a bovine serumalbumin (BSA) derivatisation by Li et al.[44], its labelling with ^{99m}Tc, and gives an introduction to the *in vitro* behaviour of the labelled and unlabelled HYNIC-DAPI derivatives in an FRTL5 cell line. Furthermore, these results provide a basis for DNA binding experiments, survival studies in cell culture, and dosimetric calculations based on the ^{99m}Tc distribution within various cell compartments.

2 Results

2.1 Chemistry

The fluorochrome DAPI was derivatised on the 3-position of the phenylindole residue by treatment with 2-hydroxy-5-nitrobenzyl bromide (Koshland's reagent). Afterwards, the palladium catalysed reduction of the nitro group gives compound **1** (Scheme 1-I)[44]. Then, 5-(*N'-tert*-butoxycarbonylhydrazino)pyridine-2-carboxylic acid 2,5-dioxo-pyrrolidin-1-yl-ester (succinimidyl-*N*-Boc-HYNIC) was reacted with 4-aminobutyric acid (GABA) in the presence of the base *N*,*N*-diisopropylethylamine (Hünig's base) to introduce the linker for coupling with **1**(Scheme 1-II). Coupling between **1** and **2** was achieved

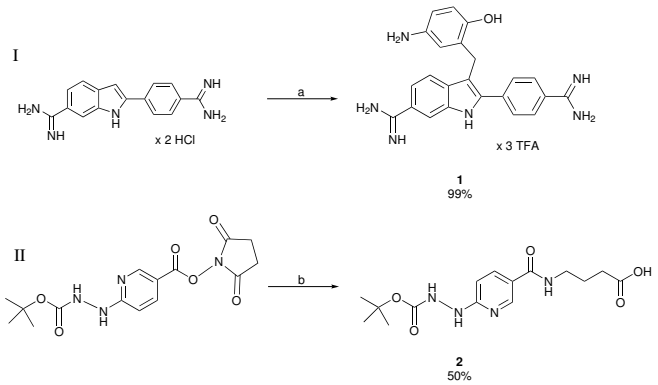

Scheme 1 Synthesis of compounds **1** and **2**. (a) 1. Koshland's reagent, water, acetone, room temperature, 1 d: 2. formic acid, 10% PdC , TFA , water, 100°C, 1 d; (b) GABA, Hünig's base, DMF, room temperature, 1 d.

by activation of the carboxylate group of **2** using 1,1'-carbonyldiimidazole (CDI) to give **3** in 14% yield after reversed phase high performance liquid chromatography (RP-HPLC) purification (Scheme 2-III). After deprotection and reprotection of **3** by treatment with trifluoroacetic acid (TFA) for 1 d, the trifluoroacetyl protected HYNIC-DAPI (**4b**) was formed as 9:1 inseparable mixture with deprotected HYNIC-DAPI (**4a**). These mixture can be used for ^{99m}Tc labelling without further purification. The deprotection with 4 M hydrochloric acid (HCl) gives the hydrochloride salt of HYNIC-DAPI (**4c**). The purification of **4c** was tedious, associated with a loss of yield, and inseparable side products were formed.

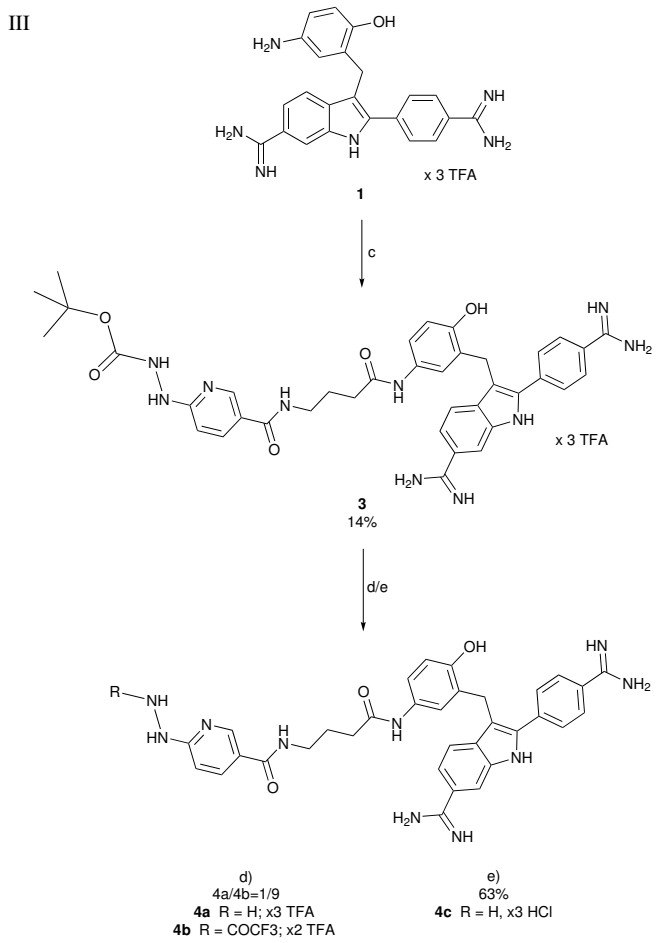

Scheme 2 The synthesis of the new HYNIC-DAPI conjugate. (c) **2**, CDI, DMF, room temperature, 1 d; (d) TFA, room temperature, 1 d; (e) 4 M HCl, room temperature, 1 h.

2.2 Radiochemistry

Both **4a**/**4b** and **4c** can be labelled using ^{99m}Tc-pertechnetate in the presence of tin(II) chloride dihydrate and tricine as coligand in saline to give ^{99m}Tc(tricine)$_n$HYNIC-DAPI (Figure 2). The reaction is complete after an incubation time of 10-15 min at room temperature and leads to a specific activity of up to 0.30 GBq/nmol. The analysis with RP-HPLC showed that the labelling of both derivatives resulted in the same product, whose formal structure is shown in Figure 1(**5**), hereafter named ^{99m}Tc-HYNIC-DAPI. The RP-HPLC chromatogram of labelled **4c** and **4a**/**4b** (1/9) is shown in Figure 2A and Figure 2B, respectively. The assignment of the most important signals from the UV traces is as follows: signal 1) HYNIC-DAPI derivatives **4c** and **4a**, signal 2) trifluoroacetyl protected HYNIC-DAPI derivative

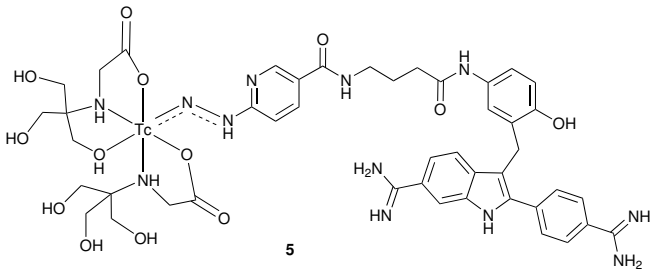

Fig. 1 Proposed structure of ^{99m}Tc(tricine)$_n$HYNIC-DAPI with HYNIC as a monodentate ligand.

(**4b**). All further UV-signals are caused by side products. The signal of ^{99m}Tc-HYNIC-DAPI was broadened, which was not unexpected. The comprehensive analysis led to the conclusion that within a retention time of 1 min up to three radioactive signals overlapped. They belong to different species of ^{99m}Tc-HYNIC-DAPI. However, they could not be separated by solid phase extraction (SPE), thin layer chromatography (TLC), or RP-HPLC.

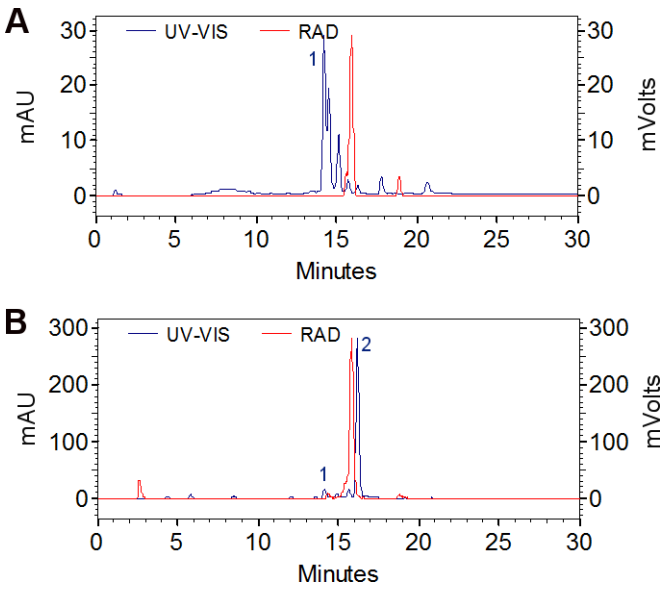

Fig. 2 RP-HPLC chromatograms of the labelled HYNIC-DAPI derivatives **4c** (A) and **4b** (B). Signal 1: HYNIC-DAPI derivatives **4c** and **4a**, signal 2: trifluoroacetyl protected HYNIC-DAPI derivative (**4b**). Detection was realized by UV- (–, 220 nm) and a Gamma-Counter (–). Monitoring was achieved by a gradient method with the eluents water and ACN, both with 0.1% TFA: 100-70% water in 30 min, flow rate 1.4 ml/min.

Radioactive impurities were detected by instant thin layer chromatography (ITLC-SG), which showed

16.5 ± 11.0% of unreduced ^{99m}Tc-pertechnetate together with an inseparable unknown ^{99m}Tc degradation product, some reduced hydrolysed ^{99m}Tc (colloid) below 6%, and 10.1 ± 7.6% of ^{99m}Tc-tricine coligand complex after 15 min reaction time. ^{99m}Tc-HYNIC-DAPI (**5**) was purified by RP-HPLC and used for *in vitro* experiments in FRTL5 cell culture.

2.3 In vitro studies

2.3.1 The properties of unlabelled HYNIC-DAPI in cell culture. The investigation of the spectral characteristics of HYNIC-DAPI in comparison to DAPI showed, that absorption and fluorescence characteristics did not change significantly and that the new derivative could be detected with the common microscope filter for DAPI. The absorption maximum, as well as the fluorescence maximum of HYNIC-DAPI, are slightly red shifted. Hence, excitation for live cell microscopy had to be higher than for DAPI but the basic characteristics remained.

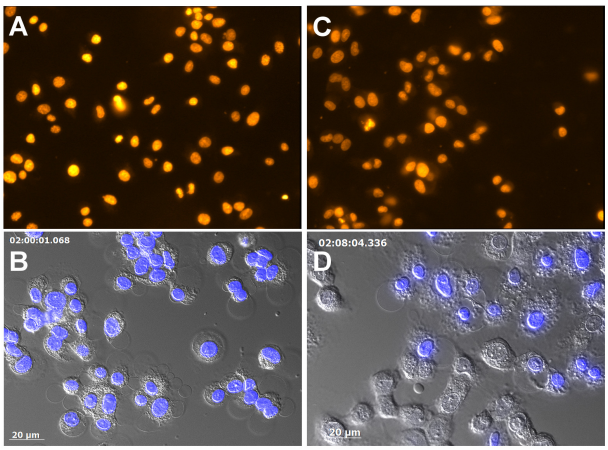

Fig. 3 Distribution characteristics of DAPI (A, B) in comparison with unlabelled HYNIC-DAPI (C, D) in FRTL5 cells. The fluorescence images A and C were recorded with the DAPI filter of an Axioskop 40 microscope (Zeiss) and show the cell nuclei of fixed cells. The live cell images (B, D) show the correlation of differential interference contrast (DIC) technique and DAPI filter (Axio Observer Z.1 microscope from Zeiss).

The addition of 20 µg DAPI ($5.7 \cdot 10^{-8}$ mol) or HYNIC-DAPI (**4a**/**4b**=1/9, $2.8 \cdot 10^{-8}$ mol) to FRTL5 cells resulted in the distribution pattern shown in Figure 3. The fluorescence micrographs A and C show the distribution within fixed cells, whereas B and D show the live cell images of DAPI (A, B) and HYNIC-DAPI (C, D). Image A and B in Figure 3 show the typical fluorescence characteristics of DAPI with high fluorescence in cell nuclei and no fluorescence enhancement in the cytoplasm. Both images led to the conclusion that the fluorescence enhancement is restricted to the nuclei and was inhomogeneous, with different fluorescence enhancement from cell to cell. The live cell experiments also showed that the fluorescence increased steadily up to 2 h (Figure 4A). At this time all nuclei are dyed (Figure 3B) and

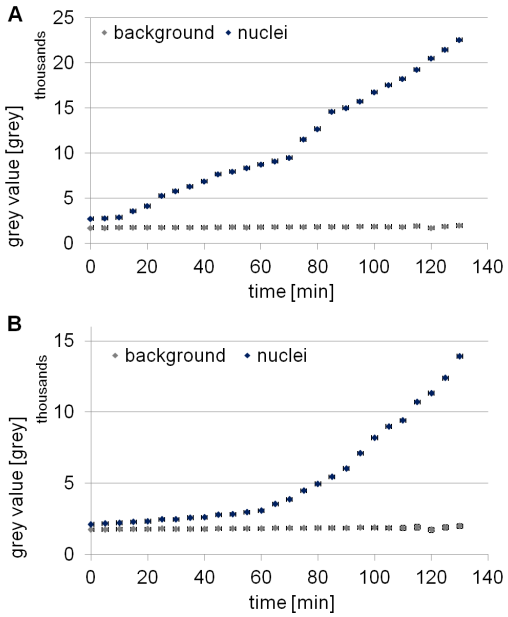

Fig. 4 The time-based changes of the fluorescence within the nuclei of DAPI (A) and HYNIC-DAPI (B) in living FRTL5 cells. The measurements with HYNIC-DAPI were determined with a higher excitation energy than for DAPI.

there is no significant difference to the results of 3A with fixed cells. The distribution pattern of HYNIC-DAPI in Figure 3C and 3D shows comparable characteristics as described for DAPI. Again, the elevation of the fluorescence signal in the nuclei is much higher than in the cytoplasm. It seemed to be steady (Figure 4B) and the fluorescence enhancement within the nuclei is also inhomogeneous as described for DAPI before. After 2 h, not all cell nuclei in the live cell experiment are dyed (4D), whereas the enrichment within the nuclei of fixed cells (4C) is more homogeneous and dyes all cell nuclei. All experiments with fixed cells showed a faster and much higher fluorescence enhancement within the nuclei than the live cell experiments. High enough to account for exclusive enrichment in nuclei as it was expected after fenestration of the cell membrane. The argument was solely qualitative because we neither quantified the elevation in quantum yield, nor distinguished if this elevation was caused by en-

hanced accumulation within the nuclei or by increasing interaction with DNA. The time-fluorescence graphs in Figure 4 gave more information about the changes in fluorescence in living FRTL5 cells over the entire measuring time. Background fluorescence is negligible in comparison to that within the nuclei. The first changes in fluorescence within the nuclei were measured after 15 min for DAPI (4A) and 25 min for HYNIC-DAPI (4B). Then, a steady fluorescence elevation for both dyes over the entire measuring time occurs and the qualitative fluorescence increase of DAPI is higher and faster compared with that of HYNIC-DAPI. The results gave no evidence about the uptake kinetics of both dyes and the changes in fluorescence quantum yield between DAPI and HYNIC-DAPI within the cell nuclei are not comparable. The fluorescence elevation proved the enrichment of both dyes within the nuclei of living FRTL5 cells and is an evidence for the local interaction with biological structures, *e.g.* the DNA.

2.3.2 The properties of ^{99m}Tc-HYNIC-DAPI in cell culture. To perform the *in vitro* experiments, an activity of 0.2 MBq of purified ^{99m}Tc-HYNIC-DAPI was given to each well. The uptakes within the cells for method 1 and method 2 are given in %. The cell uptake for method 2 was calculated as the sum of the fractions from the nuclei isolation kit. The uptakes were calculated based on the added activity of 0.2 MBq and normalised to $5 \cdot 10^5$ FRTL5 cells. The relative compartment uptake for method 2 was calculated based on the entire cell uptake and normalised to 1. All results are decay corrected and, because of the unspecific adsorption of ^{99m}Tc-HYNIC-DAPI, also background corrected.

The *in vitro* behaviour was investigated by two different methods. After the respective incubation times (see Section 5.3) cells were washed twice with cold phosphate buffered solution (PBS) and either detached with sodium hydroxide (method 1) or separated and fractionated with buffer from the Nuclei EZ Prep nuclei isolation kit (nuclei isolation kit) (method 2). Using method 1, the results showed a fast accumulation of 1.85 ± 1.09% within one hour after addition of ^{99m}Tc-HYNIC-DAPI (**—**Figure 5A). Up to 24 h the uptake slows down and reaches a maximum uptake of 2.81 ± 0.61%. The results of the preparation with the nuclei isolation kit (method 2) confirmed these observations. The experiments showed rapid accumulation within 30 min (1.89 ± 0.33%) and uptakes of 3.10 ± 0.36% after an incubation time of 24 h (— Figure 5A). Figure 5B shows the relative ratio of lysate- and nuclei-bound activity, normalised to the cell uptakes shown in Figure 5A (— method 2). Compared to the increasing cell uptakes the relative amount of nuclei bound activity remains constant. Thus, the cell fragmentation indicates that during the entire measurement period of 24 h about 1/15 of the cell internalised activity is located within the nucleus. Based on these results, the changes in cell uptake were mainly caused by the cytoplasm bound activity.

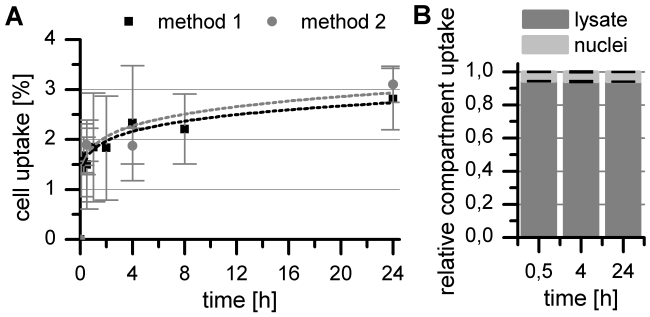

Fig. 5 A: Internalisation characteristics of ^{99m}Tc-HYNIC-DAPI. Method 1(**—**): cells detached with sodium hydroxide, method 2(—): cells treated with nuclei isolation kit. B: Relative distribution pattern of ^{99m}Tc-HYNIC-DAPI from compartmental analysis (method 2) based on the cell uptake.

2.4 Stability experiments

Stability experiments were performed with ^{99m}Tc-HYNIC-DAPI in labelling solution at room temperature at pH 5 and in Gibco F12 culture media at 37°C at pH 7 over an incubation time of 24 h (Figure 6). The decomposition half live of ^{99m}Tc-HYNIC-DAPI derivatives in the labelling solution is comparable with that in culture medium and average 8 h. After 24 h an amount of 16.00 ± 7.08% or 20.56 ± 7.01% of the original compound remains in the labelling solution or in culture

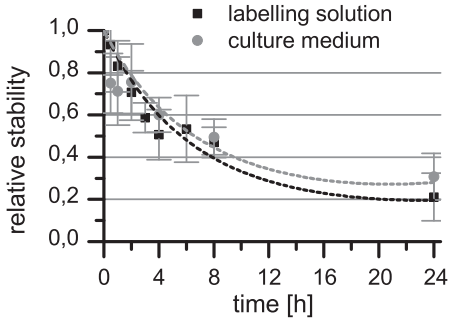

Fig. 6 Stability of ^{99m}Tc-HYNIC-DAPI derivatives in labelling solution (pH 5, room temperature) and culture medium (pH 7.2, 37°C) over incubation times of 24 h.

medium. Radioactive decomposition products were detected by TLC. They were identified as reduced hydrolysed ^{99m}Tc (colloid), free ^{99m}Tc-tricine coligand complex, and an unknown ^{99m}Tc species. However, they could not separated by SPE or RP-HPLC.

3 Discussion

3.1 Chemistry

After derivatisation of DAPI with Koshland's reagent and reduction of the nitro-group, the introduction of the HYNIC chelator to compound **1** was feasible by coupling with **2**, which was synthesised from succinimidyl-*N*-Boc-HYNIC and GABA. The final *tert*-butyloxycarbonyl (Boc) deprotection with TFA gave the new HYNIC-DAPI conjugate as a 1:9 mixture of HYNIC-DAPI **4a** and the trifluoroacetyl protected HYNIC-DAPI **4b**. When hydrochloric acid was used, complete deprotection of HYNIC-DAPI **4c** was achieved. During purification of **4c**, side products were formed that could not be separated from the product. In accordance with the literature we found, that HYNIC-DAPI is not stable in aqueous solution due to the high reactivity of the hydrazine group. HYNIC reacts with impurities that were extracted from various plastic materials and the resulting hydrazone derivatives block the labelling reaction[45]. To overcome this problem we used the more stable trifluoroacetyl protected HYNIC-DAPI **4b**, instead of the free hydrazine form **4c** or **4a**.

3.2 Radiochemistry

As described in section 2.2, the labelling of both HYNIC-DAPI derivatives **4c** and **4b** led to the same product: ^{99m}Tc-HYNIC-DAPI (**5**). There is no need for removing the TFA-group, whose advantages and characteristics already were described by Surfraz et al. for the ^{99m}Tc labelling of other trifluoroacetyl protected HYNIC derivatives[46,47]. The RP-HPLC analysis showed several ^{99m}Tc species with very similar properties, which contributed to the radioactive signal of **5** (Figure 2). The overlapping signals were expected and were caused by an coordination isomerism of the hydrazine bond of the HYNIC residue and the coligand tricine. Although literature describes that HYNIC can act as a monodentate as well as a bidentate ligand and the number of coligands can vary between 1-3, the exact coordination and configuration of ^{99m}Tc-coligand-HYNIC complexes is not known[46,48,49].

3.3 In vitro studies

3.3.1 The properties of unlabelled HYNIC-DAPI in cell culture. The distribution characteristics shown in Figure 3A and 3B led to the conclusion that DAPI was enriched in cell nuclei of living FRTL5 cells, as described in literature for other cell lines. It is also known that the fluorescence quantum yield of DAPI in aqueous solution is negligible[26,50] and that the remarkable increase of fluorescence quantum yield is caused by an AT-selective minor groove binding to DNA[26,29,31,50]. The results in 3A and 3B prove, that enrichment of DAPI in the nuclei of fixed and living FRTL5 cells goes along with an interaction with the DNA. The images in Figure 3C and 3D showed that also the unlabelled HYNIC-DAPI (**4a**/**4b**) is able to cross the cell membranes of living FRTL5 cells. Furthermore, a qualitative analysis demonstrated a higher elevation of fluorescence in nuclei than in the cytoplasm for both dyes (Figure 4). In comparison with DAPI, the fluorescence signal of HYNIC-DAPI in aqueous solution is insignificant. Therefore it is likely that the enrichment in the nuclei is also related to an interaction with the DNA of living FRTL5 cells. The measurements gave no information about the kinetics of internalisation of DAPI and HYNIC-DAPI. No uptake information of DAPI is given in the literature. The change of the quantum yield indicated the interaction of both dyes with biological structures, *e.g.* the DNA, but did not allow to determine the quantitative uptake into cell compartments. The changes in fluorescence enhancement of both dyes, as seen in Figure 4, were not comparable. As described in literature, the fluorescence quantum yield depends on the composition of the DNA, e.g. the conformation or the AT content, thereby on the disposability of binding sites, and the type of interaction[28–33]. This is one reason why the fluorescence intensity within the cell nuclei seemed inhomogeneous for both dyes. Furthermore, the enrichment within the cell nuclei is dependent on involved transport mechanisms during influx, efflux, and on cell specific decomposition mechanisms. Up to date the transport routes and the metabolism of DAPI were mainly unresolved, but it was assumed that multitude pathways are involved[51,52]. The efficiency of decomposition and transport mechanisms of DAPI and HYNIC-DAPI may be dependent on the individual state of the cells, e.g. the vitality, the integrity of cell membranes, extraneous influences, and the phase of the cell cycle. These influences to the *in vitro* behaviour may also cause the inhomogeneous enrichment.

The requirement for the comparison of DAPI and HYNIC-DAPI in Figure 4 is the knowledge of the affinity, the binding mode, and the individual factor for the

enhancement of the fluorescence quantum yield for the special interaction with the DNA of FRTL5 cells. So far, we were not able to quantify the elevation in quantum yield in the nuclei of living FRTL5 cells, but the qualitative studies suggests an interaction between HYNIC-DAPI and DNA as described for DAPI before. The investigation of the of the HYNIC-DAPI derivatives with calf thymus DNA (ctDNA) will be investigated in further studies, first results of the effects of ^{99m}Tc-HYNIC-DAPI on plasmid DNA have already been published[13].

3.3.2 The properties of ^{99m}Tc-HYNIC-DAPI in cell culture. Uptake experiments showed that ^{99m}Tc-HYNIC-DAPI is able to cross the cell membranes of living FRTL5 cells and correlated with the qualitative fluorescence data. The inability to characterise the ^{99m}Tc species of HYNIC-DAPI is not unexpected[46,48,49], but does create problems in understanding which radiochemical species may be responsible for cell uptake and internalisation into the nuclei. The comparison of the uptake results, obtained with two different methods, showed good correlation within an incubation time of 24 h. The determined uptake maxima were at 2.81 ± 0.61% with method 1 and 3.10 ± 0.36% with method 2 (Figure 5A). Furthermore, both methods showed that the accumulation within 1 h is initially fast and then slows down. This seemed to be a strange uptake pattern and indicated the influence of interfering parameters. From our point of view the most important parameter is the unspecific adsorption of the ^{99m}Tc-HYNIC-DAPI species to the plastic wells which also caused the large error bars. Hence, reference measurements were performed and all uptakes were background corrected. Based on the results of the compartment analysis (nuclei isolation kit, method 2), the amount within the nuclei is an average 1/15 of the cell-internalised activity. Although ^{99m}Tc-HYNIC-DAPI showed enrichment and distribution within the whole cells, it cannot be considered to be specific for an interaction with the DNA of living FRTL5 cells. Further investigations of our group confirm the thesis of a direct interaction with free DNA and proof that ^{99m}Tc-HYNIC-DAPI is bound to plasmid DNA, introducing 4-fold more single-strand breaks (SSB) and up to 10-fold more double-strand breaks (DSB) than free ^{99m}Tc sodium pertechnetate[13].

As shown in section 2.4 the decomposition half life of ^{99m}Tc-HYNIC-DAPI is about 8 h in culture medium. Decomposition influences the internalisation into the cells and the distribution between the cell compartments, *e.g.* into the nuclei. Therefore, the limited disposability of ^{99m}Tc-HYNIC-DAPI could be the explanation for the decreasing uptake kinetic from 1-24 h and the constant amount of activity within the cell nuclei. It is likely that the plateau in the uptake curve (Figure 5A) is caused by the stopped internalisation of ^{99m}Tc-HYNIC-DAPI and the residue of the decomposition products within the cell compartments. This means the decomposition products neither internalise into cells nor move within the cell compartments. The influence of ^{99m}Tc sodium pertechnetate is negligible because all uptake experiments were achieved with purified ^{99m}Tc-HYNIC-DAPI. The internalisation of reduced hydrolysed ^{99m}Tc (colloid) in cells is not considerable. The uptakes of the ^{99m}Tc-tricine coligand complex and of the unknown ^{99m}Tc decomposition products could be approximately determined from the other decomposition products. The measurements with reference preparations suggest that the uptake of these products is negligible and that there is no enrichment into cell nuclei (data not shown). Possible and up to date unknown further impairments of the *in-vitro* behaviour are cell specific decomposition mechanisms and influences of involved transport mechanisms, as described in section 3.3.1.

3.4 Stability

The experiments showed a lower stability of ^{99m}Tc-HYNIC-DAPI (**5**), as expected. In further investigations, the use of another coligand may give a higher stability of the complex that may finally result in higher uptake. The stability of the complex with tricine as coligand in the labelling solution is comparable with that in culture medium. After approximately 1 d, ≤ 20% of intact complex was detected. Three species of decomposition products were identified by ITLC-SG: reduced hydrolysed ^{99m}Tc (colloid), ^{99m}Tc-tricine coligand, and one unknown ^{99m}Tc species. The characterisation of the ^{99m}Tc-tricine coligand species and the unknown decomposition products of ^{99m}Tc-HYNIC-DAPI was not possible because they could not be isolated by SPE or RP-HPLC.

4 Conclusion

A new HYNIC-DAPI derivative for labelling with the radio nuclide ^{99m}Tc was successfully designed. The labelling procedure is a simple batch preparation that leads to high specific activity. The fluorescence micrographs and several *in vitro* experiments proved that the labelled as well as the unlabelled HYNIC-DAPI derivatives were able to cross different cell barriers and enrich within the nuclei of living FRTL5 cells. The enrichment may be influenced or limited by various parameters, *e.g.* stability, the isomerism of the coligand complex, the un-

specific adsorption, together with cell specific decomposition and transport mechanisms. No reference data about uptake mechanisms and the distribution ratio of DAPI in living cells are available so far, which creates problems in understanding the *in vitro* behaviour of the new HYNIC-DAPI derivative. To overcome these limitation, further experiments with DAPI and HYNIC-DAPI in other cell lines could offer a better understanding of the internalisation mechanism. Moreover, the low stability of ^{99m}Tc-HYNIC-DAPI limits the accumulation rate and may be improved by another coligand which may lead to higher cell or nuclei uptakes. Furthermore, the unlabelled and the labelled HYNIC-DAPI are similar in their (bio)chemical properties and *in vitro* behaviour. The qualitative analysis of the experiments with fixed and living cells indicated an enrichment within the cell nuclei by shifting the quantum yield and confirmed the results of the uptake measurements. As mentioned before, we neither quantified the elevation in quantum yield nor determined the binding mode in the HYNIC-DAPI-DNA complexes.

The new HYNIC-DAPI derivative gives no ability for any therapeutic use in auger emitter radiotherapy. Neither DAPI nor HYNIC-DAPI are selective for a cell line or a special tumour tissue. The goal of this work was the development of a multifunctional compound with DAPI as a carrier for ^{99m}Tc, the radiolabelling, and the *in vitro* evaluation in an FRTL5 cell line. These results provide a basis for the quantification of radiotoxic effects and dosimetric parameters for the damaging potential of an auger emitter under *in vitro* conditions.

5 Experimental section

5.1 Chemistry

All reagents and solvents were purchased from Appli Chem, TCI, Fluka, Merck, and Sigma Aldrich. 6-Boc-hydrazinopyridine-3-NHS was synthesised as described in the literature[40]. All chemical reagents were of highest commercially available quality and were used without further purification. Analytical high performance liquid chromatography (HPLC) analyses for compounds **1**, **2**, **3**, and **4** were performed using an Agilent 1100 HPLC (Agilent Technologies, Böblingen/Baden-Württemberg/Germany) with a quaternary pump, UV/Vis detector, and autosampler. For compound **1**-**3** and **4a**/**4b** the system was equipped with a Sunfire® C18 column (4.6 x 250 mm, 5 µm). Monitoring was achieved by a gradient method with the eluents water and acetonitrile, both with 0.1% TFA: 100-60% water (0-30 min), 60-30% water (30-40 min), flow rate 1 ml/min. UV detection was performed at wavelengths of 220, 280, 308, and 326 nm. The analytical system for compound **4c** was equipped with a YMC ODS-A C18 column (4.6 x 250 mm, 5 µm). Monitoring was achieved by a gradient method with the eluents water and acetonitrile, both with 0.1% 12 M HCl: 100-60% water (0-30 min), flow rate 1 ml/min. UV detection was set at 220 nm. BocHYNIC-DAPI **3** and deprotected HYNIC-DAPI **4c** were purified by preparative HPLC (Merck-Hitachi LaChrome D-7000) with an L-7100 pump and an L-7400 UV detector (Merck, Darmstadt/Hesse/Germany). The system was equipped with a Sunfire® Prep C18 OBD column (30 x 250 mm, 10 µm). The eluents for purifying **3** were water and acetonitrile, both with 0.1% trifluoroacetic acid (TFA): 20% acetonitrile, isocratic conditions, flow rate 20 ml/min. UV detection was set at 220 nm. Purification of **4c** was achieved with the eluents water and acetonitrile, both with 0.1% 12 M HCl: 100-60% water (0-40 min), flow rate 20 ml/min, UV detection was set at 220 nm.

^{1}H-NMR and ^{13}C-NMR spectra were recorded with a Bruker spectrometer (Bruker BioSpin GmbH, Rheinstetten/Baden-Württemberg/Germany) in deuterated dimethyl sulfoxide (DMSO-d_6) or deuterated methanol (CD_3OD). The chemical shifts are reported in parts per million (ppm), and the coupling constants (J) are reported in hertz (Hz). The centre lines of the multiplets of dimethyl sulfoxide (DMSO) or CD_3OD were defined as 2.5, respectively 3.3 ppm and were used as internal references for the ^{1}H-nuclear magnetic resonance (NMR) spectra. electro spray ionisation mass spectra (ESI-MS) were obtained using a MSQ mass detector (Thermo Fisher Scientific, Waltham/Massachusetts/USA).

^{99m}Tc labelling was performed with fresh eluate from a ^{99}Molybdenum (^{99}Mo)/^{99m}Tc generator (Ultra-Technekow^{TM} FM, Covidien, Neustadt a. d. Donau/Bayern/Deutschland). Analysis and purification of the labelling products were performed using a Merck Hitachi Elite La Chrome HPLC instrument consisting of a pump, a L2420 UV-Vis detector, and a L2300 column oven (Merck, Darmstadt/Hesse/Germany). The system was equipped with a Chromolith® Performance HPLC column RP18e (100 x 4.6 mm, 5 µm). The monitoring and purification of the labelling products were achieved under two different methods. The eluents were water and acetonitrile, both with 0.1% trifluoroacetic acid. The UV detection was set at 220 nm. Monitoring: 0-30% acetonitrile (0-30 min), flow rate 1.4 ml/min. Purification: 11-16% acetonitrile (0-20 min), flow rate 1.2 ml/min.

TLC was performed with ITLC-SG (Varian) with

saline, 2-butanone and a mixture of acetonitrile/water/trifluoroacetic acid 2/2/0.1 (v/v/v) as solvents. The chromatography paper was analysed with a VCS 203 scanner from Veenstra (version 2.01). All radioactive samples from the *in vitro* experiments were measured with the Isomed 2000 V1.22 (MED Nuklearmedizintechnik Dresden GmbH, Dresden/Saxony/Germany) or with the gamma-counter COBRA^{TM}II Auto-Gamma (Packard).

5.1.1 3-(5-Amino-2-hydroxybenzyl)-2-(4-carbamimidoylphenyl)-1*H*-indole-6-carboxamidine TFA salt (1). Step 1: 2.85 mmol of 4,6-diamidin-2-phenylindole dihydrochloride (1.00 g, 1 eq.) was dissolved in 50 ml water and 27 ml acetone. A solution of 1.2 eq. Koshland's reagent (3.45 mmol, 0.80 g) in 27 ml acetone was added and the mixture was stirred at room temperature. After 22 h a second portion of 0.2 eq. Koshland's reagent (0.69 mmol, 0.16 g) was added and the reaction mixture was stirred for another 22 h. Then, the solvents were evaporated and the residue was dissolved in methanol. The mixture was evaporated again, the resulting yellow precipitate was suspended in chloroform and stirred overnight. The solid was filtered, washed twice with chloroform and once with water to give 61% (1.73 mmol, 0.74 g) of product.
Analytical HPLC: retention time (t_R)=22.2 min.
δ_H (CD_3OD, 500 MHz) [ppm] 8.05 (s, 1 H), 8.00 (dd, ^3J=8.9 Hz, ^4J=2.7 Hz, 1 H), 7.93 (d, ^3J=8.3 Hz, 2 H), 7.85 (d, ^3J=8.3 Hz, 2 H), 7.63 (d, ^3J=8.4, 1 H), 7.56 (d, ^4J=2.5 Hz, 1 H), 7.46 (dd, ^3J=8.4 Hz, ^4J=1.1 Hz, 1 H), 6.97 (d, ^3J=8.9 Hz, 1 H), 4.33 (s, 2 H).
δ_C (CD_3OD, 126 MHz) [ppm] 169.43, 162.93, 141.89, 139.80, 139.07, 137.53, 134.71, 129.86, 129.83, 129.59, 129.20, 125.69, 125.08, 123.23, 121.14, 119.79, 115.70, 113.47, 112.51, 25.09.
Step 2: 1.26 mmol (0.63 g, 1 eq.) product from step 1 was solved in 71 ml formic acid. Then 2.70 g 10% Pd/C and 23.7 ml of a 1:1 mixture of trifluoroacetic acid and water were added successively. The reaction mixture was heated to 100°C for 18 h. It was filtered through celite, the residue was washed with formic acid, and the filtrate was evaporated to yield 99% (1.24 mmol, 0.92 g) of a yellow solid.
Analytical HPLC: t_R=16.3 min.
δ_H (CD_3OD, 500 MHz) [ppm] 8.06-8.11 (m, 3 H), 8.03 (d, ^4J=1.3 Hz, 1 H), 7.92 (d, ^3J=8.6 Hz, 2 H), 7.85 (d, ^3J=8.6 Hz, 2 H), 7.62 (d, ^3J=8.4 Hz, 1 H), 7.45 (dd, ^3J=8.5 Hz, ^4J=1.7 Hz, 1 H), 7.04 (dd, ^3J=8.6 Hz, ^4J=2.8 Hz, 1 H), 6.95 (d, ^3J=8.6 Hz, 1 H), 6.75 (d, ^3J=2.7 Hz, 1 H), 4.31 (s, 2 H).
δ_C (CD_3OD, 126 MHz) [ppm] 169.12, 162.58, 157.09, 139.76, 138.98, 137.60, 134.92, 130.54, 129.80, 129.79, 129.70, 129.12, 124.43, 123.33, 122.96, 122.88, 121.26, 119.64, 116.75, 113.34, 113.06, 25.16.

5.1.2 4-{[6-(*N*'-*tert*-Butoxycarbonyl-hydrazino)-pyridine-3-carbonyl]-amino}-butyric acid (2). A 2.85 mmol (0.29 g, 1 eq) sample of GABA was dissolved in 12 ml *N*,*N*-dimethylformacmide (DMF), then 4 eq. (11.47 mmol, 1.95 ml) Hünig's base and 1 eq. (2.85 mmol, 1.00 g) succinimidyl-*N*-Boc-HYNIC were added. The reaction mixture was stirred for 23 h at room temperature. DMF was evaporated and the product was dried over night to obtain a yellow oil. The crude product was purified by column chromatography with methylene chloride/ethyl acetate/methanol 5/5/1 (v/v/v) to afford **2** as a white solid in 50% yield (1.43 mmol, 0.48 g).
Analytical HPLC: t_R=18.6 min.
δ_H (DMSO-d_6, 500 MHz) [ppm] 12.03 (br s, 1 H), 8,92 (br s, 1 H), 8.65 (s, 1 H), 8.53 (d, ^4J=1.6 Hz, 1 H), 8.29 (t, ^3J=5.4 Hz, 1 H), 7.94 (d, ^3J=8.7 Hz, 1 H), 6.50 (d, ^3J=8.8 Hz, 1 H), 3.24 (dd, ^2J=12.7 Hz, ^3J=6.7 Hz, 2 H), 2.26 (t, ^3J=7.3 Hz, 2 H), 1.68-1.76 (m, 2 H), 1.42 (s, 9 H).
δ_C (DMSO-d_6, 126 MHz) [ppm] 165.04, 161.61, 155.86, 147.79, 136.64, 120.59, 104.63, 79.24, 38.50, 31.30, 28.16, 24.70.

5.1.3 *N*'-[5-(3-{3-[6-Carbamimidoyl-phenyl)1*H*-indol-3-ylmethyl]-4-hydroxyphenylcarbamoyl}-pyridin-2-yl]-hydrazinecarboxylic acid tert-butyl ester TFA salt (3). A 1.23 mmol (0.91 g, 1 eq.) sample of compound **2** was dissolved in 12.6 ml DMF. Then 1 eq. of CDI (2.29 mmol, 0.37 g) were added and the mixture was stirred for 1 h under exclusion of light. Afterwards, 1.85 eq. of **1** (2.29 mmol, 0.77 g) in 7 ml DMF was added dropwise to the solution of **2** and the reaction mixture was stirred for 24 h under exclusion of light at room temperature. The solvent was removed, the residue was purified by preparative HPLC and dried over night to yield 14% (0.18 mmol, 0.19 g) of a yellow solid.
Analytical HPLC: t_R=26.2 min.
δ_H (DMSO-d_6, 500 MHz) [ppm] 12.23 (s, 1 H), 9.45 (s, 2 H), 9.34 (s, 2 H), 9.23 (s, 2 H), 9.22 (s, 3 H), 9.04 (br. s, 1 H), 8.99 (s, 3 H), 8.47 (d, ^4J=1.8 Hz, 1 H), 8.30 (s, 1 H), 7.97-7.89 (m, 2 H), 7.95 (d, ^3J=8.3 Hz, 2 H), 7.83 (d, ^3J=8.5 Hz, 2 H), 7.57 (d, ^3J=8.4 Hz, 1 H), 7.41 (dd, ^3J=8.5 Hz, ^4J=1.3 Hz, 1 H), 7.36 (dd, ^3J=8.6 Hz, ^4J=2.4 Hz, 1 H), 6.82 (d, ^4J=2.3 Hz, 1 H), 6.80 (d, ^3J=8.7 Hz, 1 H), 6.59 (d, ^3J=8.0 Hz, 1 H), 4.15 (s, 2 H, H-9), 3.16 (dd, ^3J=6.2 Hz, ^2J=13.2 Hz, 2 H), 2.13 (t,

^3J=7.4 Hz, 2 H), 1.62-1.71 (m, 2 H), 1.42 (br s, 9 H).
δ_C (DMSO-d_6, 126 MHz) [ppm] 169.95, 166.36, 165.00, 164.54, 155.70, 150.73, 146.44, 137.48, 136.69, 135.44, 135.04, 132.81, 131.18, 128.72, 127.75, 127.28, 126.47, 121.37, 120.57, 119.77, 119.53, 119.00, 118.59, 118.56, 118.45, 114.52, 112.18, 112.03, 79.42, 38.65, 33.56, 28.06, 25.22, 24.12.
† *m/z* $[M+H]^+$ 719.3, calculated 719.3; $[M+TFA-H]^-$ 831.5, calculated 831.3.

5.1.4 *N*-(4-(3-((6-carbamimidoyl-2-(4-carbamimidoylphenyl)-1*H*-indol-3-yl)methyl)-4-hydroxyphenylamino)-4-oxobutyl)-6-(2-(2,2,2-trifluoracetyl)hydrazinyl)nicotinamide TFA salt (4b). A 0.05 mmol (0.05 g) sample of BocHYNIC-DAPI (**3**) was dissolved in trifluoroacetic acid. The reaction mixture was stirred for 22 h under the exclusion of light at room temperature. The solvent was evaporated, the residue was dissolved in diethyl ether and stirred for 2 h at room temperature. Afterwards, the solvent was removed and the residue was washed twice with diethyl ether. The product was evaporated and dried. 36 mg (0.05 mol) of compound **4** were obtained as a 1:9 mixture of HYNIC-DAPI (**4a**) and trifluoroacetyl protected HYNIC-DAPI (**4b**).
Analytical HPLC: t_R(**4b**)=20.7 min.
δ_H (DMSO-d_6, 500 MHz) [ppm] **4b** 12.22 (s, 1 H), 9.47-9.41 (m, 2 H), 9.34 (s, 2 H), 9.23 (s, 2 H), 9.19 (s, 2 H), 8.96 (s, 2 H), 8.51 (s, 1 H) , 8.31 (t, ^3J=5.35 Hz, 1 H), 7.97-7.90 (m, 4 H), 7.83 (d, ^3J=8.37 Hz), 7.57 (d, ^3J=8.70 Hz, 1 H), 7.41 (dd, ^3J=8.40, ^4J=1.30 Hz, 1 H), 7.36 (dd, ^3J=8.53 Hz, ^4J=2.17 Hz, 1 H), 6.82 (d, ^4J=2.34 Hz, 1 H), 6.80 (d, ^3J=8.70 Hz, 1 H), 6.66 (d, ^3J=8.70 Hz, 1 H), 4.15 (s, 2 H), 3.16 (q, ^3J=6.58 Hz, 2 H), 2.13 (t, ^3J=7.36 Hz, 2 H), 1.67 (quin, ^3J=7.36 Hz, 2 H).
δ_C (DMSO-d_6, 125 MHz) [ppm] (**4b**) 176.22, 170.00, 166.34, 165.00, 164.57, 150.79, 137.54, 136.71, 135.48, 132.86, 131.24, 128.82, 127.78, 127.36, 126.52, 123.18, 121.44, 119.75, 119.61, 118.64, 118.46, 117.75, 115.42, 114.55, 112.25, 112.04, 38.70, 33.56, 25.23, 24.16.
† *m/z* (**4a**) $[M+H]^+$ 619.4, calculated 619.3; $[M+TFA-H]^-$ 731.3, calculated 731.3. (**4b**) $[M+H]^+$ 715.4, calculated 715.3; $[M+TFA-H]^-$ 827.4, calculated 827.3; $[M-H]^-$ 713.6, calculated 713.3.

5.1.5 *N*-(4-(3-((6-carbamimidoyl-2-(4-carbamimidoylphenyl)-1*H*-indol-3-yl)methyl)-4-hydroxyphenylamino)-4-oxobutyl)-6-(2-hydrazinyl)-nicotinamide hydrochloride (4c). A 0.04 mmol (0.04 g) sample of BocHYNIC-DAPI (**3**) was dissolved in 4 M HCl. The reaction mixture was stirred for 1 h under the exclusion of light at room temperature. The product was purified by preparative RP-HPLC, evaporated, and dried to yield 62.7% (0.02 mmol, 0.015 g) of a yellow solid.
Analytical HPLC: t_R=18.8 min.
δ_H (DMSO-d_6, 500 MHz) [ppm] 12.49-12.32 (m, 1 H), 9.67 (br. s., 1 H), 9.58-8.62 (m, 13 H), 8.24 (br s., 1 H), 8.06-7.74 (m, 6 H), 7.55 (d, ^3J=7.70 Hz, 1 H), 7.39 (m, 2H), 6.97-6.47 (m, 3 H) , 4.13 (br. s., 2 H), 3.63-3.05 (m, 2 H), 2.21-2.00 (m, 2 H), 1.57-1.80 (m, 2 H).
δ_C (DMSO-d_6, 125 MHz) [ppm] 169.36, 165.71, 164.32, 150.11, 148.31, 136.81, 136.04, 134.80, 132.15, 130.50, 128.12 127.10, 126.41, 125.81, 123.48, 120.56, 119.11, 119.00, 118.84, 117.87, 117.76, 113.86, 111.68, 111.26, 32.88, 25.49, 23.48.
† *m/z* $[M+H]^+$ 619.4, calculated 619.3; $[M+K]^+$ 657.2, calculated 657.3.

5.2 Radiochemistry

Labelling was achieved with $7.0 \cdot 10^{-9}$ mol HYNIC-DAPI and 2 GBq of fresh ^{99m}Tc sodium pertechnetate from a ^{99}Mo/^{99m}Tc generator system in 1.0-1.5 ml saline (Fresenius Kabi) and 200 µl of a stock solution of $1.12 \cdot 10^{-1}$ mol tricine, containing $5.32 \cdot 10^{-4}$ mol tin(II) chloride dihydrate ($SnCl_2 \cdot 2H_2O$), was added. The reaction mixture was incubated for 15 min at room temperature. After quality control by TLC the labelling product was purified by RP-HPLC and used for stability analysis or *in vitro* experiments with the FRTL5 cell culture.

5.3 Cell culture experiments

All chemicals and culture media were purchased from Invitrogen, Biochrom AG, Merck, and Sigma-Aldrich. The FRTL5 cell line was obtained from the National Centre for Radiation Research in Oncology (OncoRay, Dresden). The nuclei isolation kit was purchased from Sigma Aldrich. For the uptake experiments cells were grown in 6-well multititer plates (MTP) (Becton Dickinson). Cells for live cell microscopy were sowed in special petri dishes from Ibidi, and those for the experiments with fixed cells in LabTekII chamber slides from Nunc. All cells were grown for 1 d in a CB150 or CB150E incubator from Binder in an atmosphere containing 5% carbon dioxide at 37°C. After the addition of purified ^{99m}Tc-HYNIC-DAPI, the cells were incubated in a IG150 incubator from Jouan with 5% carbon dioxide at 37°C. Cell counting, growth control, and the analysis of fixed cells were performed with an Axioskop 40 microscope from Zeiss. For live cell microscopy, an Axio Observer Z.1 microscope by Zeiss with an incubator from Pecon was used. Both microscopes were equipped with a filter for transmitted light and a DAPI filter (λ_{Ex} 360 nm, λ_{Em} 460 nm).

5.3.1 Tissue preparation. FRTL5 cells were grown in Gibco® F12 +Gluta2MAX^{TM}-I culture medium (Invitrogen) with the following additives: 5% foetal calf serum (FCS), 10 nmol/l hydrocortisone, 5 µg/ml transferrin, 10 ng/ml somatostatine, 10 ng/ml of the amino acids glycine, histidine, and lysine, 10 mU/ml thyroid stimulating hormone (TSH), and 10 µg/µl insulin. For the uptake (6-well MTP) and live cell experiments (petri dishes), $2.5 \cdot 10^5$ cells per cavity were grown. For the experiments with fixed cells, $3 \cdot 10^5$ cells were grown in chamber slides. Before starting an experiment the culture medium was replaced with 2 ml of fresh medium, including the required amount of labelled or unlabelled HYNIC-DAPI. Reference experiments were performed with 2 ml of renewed culture medium without any additions.

5.3.2 Fluorescence microscope analysis. For the fixation experiments, $3 \cdot 10^5$ FRTL5 cells were grown for 1 d in 2 ml culture medium. Than the supernatant supernatant was removed and the cells were washed twice with 1 ml cold PBS (4°C). They were fixed with 0.5 ml of 1% formaldehyde (Sigma Aldrich) in PBS buffer for 15 min and washed three times with 1 ml PBS for 5 min at room temperature. For the permeabilisation all cells were incubated three times with 0.5 ml 0.1% Triton X-100 (Merck) in PBS buffer for 5 min at room temperature, then washed three times with 1 ml PBS for 5 min at room temperature. The pretreated cells were incubated with $1.4 \cdot 10^{-8}$ mol DAPI (5 µg) or HYNIC-DAPI (10 µg) for 1 h in 2 ml of fresh culture medium at 37°C. The cells were washed twice with 1 ml PBS at room temperature and the chamber was removed. The cells were surfaced with fluorescence mounting medium, covered with a cover glass and were analysed with the DAPI filter of the fluorescence microscope (Axioskop 40, Zeiss).
For live cell imaging, $2.5 \cdot 10^5$ cells per cavity were incubated with respectively 20 µg of DAPI ($5.71 \cdot 10^{-8}$ mol) or HYNIC-DAPI ($2.8 \cdot 10^{-8}$ mol) in 1.5 ml fresh, temperature controlled (37°C) culture medium. After each 5 min interval, images with exposure times of 20 ms (DAPI) and 350 ms (HYNIC-DAPI) were recorded with a DAPI filter. The visualisation with DIC technique was conducted simultaneous with exposure times of 50 ms. All images were recorded with the 40x-oil object lens of an Axio Observer Z.1 microscope (Zeiss). The overall measuring time lasted 2 h. Changes in fluorescence intensities were determined using the free software Fiji 1.46 and whose region of interest (ROI) manager tool. Into the cell nuclei and the background of all images respectively 1000 or 30 ROIs were located. The mean values of every image gave the fluorescence emission curve as seen in Figure 4.

5.3.3 Uptake experiments. $2.5 \cdot 10^5$ cells were grown in three of six cavities of the 6-well MTP. The remaining three cavities without cells served as references to estimate background binding. All cavities were treated similarly. Every well was incubated with 0.2 MBq of purified ^{99m}Tc-HYNIC-DAPI in 2 ml fresh, temperature controlled (37°C) culture medium and placed in the incubator. The uptake was observed over 24 h (5, 10, 15, 30 min, and 1, 2, 4, 8, 24 h). At chosen incubation times, the respective MTP were put on ice for 2 min and the supernatant was removed. All cavities were washed twice with 1 ml of cooled (4°C) PBS. Cells were detached with 1 ml of 0.1 N sodium hydroxide. All fractions were collected separately and measured with the gamma-counter. The cell uptake was calculated based on the added activity of 0.2 MBq and is given in %. It is decay, background corrected, and normalised to $5 \cdot 10^5$ FRTL5 cells.

5.3.4 Uptake experiments with cell fractionation. Six-well MTP were handled similarly as in standard uptake experiments (see Section 5.3.3). Investigations were also conducted after 5, 10, 15, 30 min, and 1, 2, 4, 8, 24 h. The respective multiwell plates were put on ice for 2 min and the supernatant was removed. Cell nuclei were separated according to the protocol for the commercially available nuclei isolation kit. All fractions were collected separately and measured with the gamma-counter.
The cell uptake was calculated from the sum of the compartment fractions based on the added activity of 0.2 MBq, is background corrected, normalised to $5 \cdot 10^5$ FRTL5 cells, and is given in %. The relative compartment uptake was calculated based on the cell uptake and normalised to 1.

5.4 Stability experiments

The stability of ^{99m}Tc-HYNIC-DAPI was investigated by TLC in the labelling solution and in culture medium after incubation times of 5, 10, 15, 30 min, and 1, 2, 4, 8, 24, and 48 h. The experiments were performed under following conditions:

1. in labelling solution: pH 5, room temperature, with no further add on;

2. in culture medium: pH 7, 37°C, dilution of 50 µl (ca. 100 MBq) of purified ^{99m}Tc-HYNIC-DAPI in 0.5 ml fresh, temperature controlled culture medium.

Both mixtures were incubated and shaken at 350 rpm at temperature control.

6 Acknowledgements

This work was supported by the European Social Fund (ESF, grant code: 080951832) and the German Research Foundation (DFG, grant code: KO1695/4-1), which are gratefully acknowledged. We thank Dr. J. Fohrer and A. Körtje from the Institute of Organic Chemistry, department of spectroscopy, from the Leipniz University of Hannover who conducted the ^{13}C-NMR measurements.

References

1 S. Jurisson, D. Berning, W. Jla and D. Ma, *Chem Rev*, 1993, **93**, 1137–1156.
2 A. I. Kassis, *Semin Nucl Med*, 2008, **35**, 358–366.
3 D. M. Lewis, *Eur J Nucl Med Mol Imaging*, 2009, **36**, 1371–1374.
4 J. Kotzerke, M. Wendisch, R. Freudenberg, R. Runge, L. Oehme, G. J. Meyer, L. A. Kunz-Schughart and G. Wunderlich, *Nuklearmedizin*, 2012, **51**, 170–178.
5 G. Wunderlich, M. Wendisch, D. Aurich, R. Runge, R. Freudenberg and J. Kotzerke, *Nuklearmedizin*, 2012, **51**, 179–185.
6 S. J. Karnas, V. V. Moiseenko, E. Yu, P. Truong and J. J. Battista, *Radiat Environ Biophys*, 2001, **40**, 199–206.
7 F. Buchegger, F. Perillo-Adamer, Y. M. Dupertuis and A. Bischof Delaloye, *Eur J Nucl Med Mol Imaging*, 2006, **33**, 1352–1363.
8 R. W. Howell, *Int J Radiat Biol*, 2008, **84**, 959–975.
9 B. Cornelissen, *J Label Compd Radiopharm*, 2014, **57**, 310–316.
10 K. G. Hofer, *Radiat Prot Dosim*, 1998, **79**, 405–410.
11 K. G. Hofer, *Acta Oncol*, 2000, **39**, 651–657.
12 A. I. Kassis, *Int J Radiat Biol*, 2004, **80**, 789–803.
13 J. Kotzerke, R. Punzet, R. Runge, S. Ferl, L. Oehme, G. Wunderlich and R. Freudenberg, *PLOS ONE*, 2014, **9**, 1–10.
14 F. M. Kievit and M. Zhang, *Adv Mater*, 2011, **23**, 217–247.
15 D. J. Hnatowich, P. J. Winnard, F. Virzi, T. Fogarasi, Sano, C. L. Smith, C. R. Cantor and M. Rusckowski, *J Nucl Med*, 1995, **36**, 2306–2314.
16 X. Liu, Y. Wang, K. Nakamura, S. Kawauchi, A. Akalin, D. Cheng and L. Chen, *J Nucl Med*, 2009, **50**, 582–590.
17 G. L. Griffiths, S. V. Govindan, G. Sgouros, G. L. Ong, D. M. Goldenberg and M. J. Mattes, *Int J Cancer*, 1999, **81**, 985–992.
18 N. Agorastos, L. Borsig, A. Renard, P. Antoni, G. Viola, B. Spingler, P. Kurz and R. Alberto, *Chem Eur J*, 2007, **13**, 3842–3852.
19 P. Haefliger, N. Agorastos, A. Renard, G. Giambonini-Brugnoli, C. Marty and R. Alberto, *Bioconj Chem*, 2005, **16**, 582–587.
20 F. Marques, A. Paulo, M. P. Campello, S. Lacerda, R. F. Vitor, L. Gano, R. Delgado and I. Santos, *Radiat Prot Dosim*, 2005, **116**, 601–604.
21 R. F. Vitor, T. Esteves, F. Marques, P. Raposinho, A. Paulo, S. Rodrigues, J. Rueff, S. Casimiro, L. Costa and I. Santos, *Cancer Biother Radiopharm*, 2009, **24**, 551–563.
22 K. Schomäcker, *Multidrug-resistente und nicht-resistente MCF-7-Mammakarzinomzellen - Vergleich der Strahlensensibilität*, 46. Jahrestagung der Deutschen Gesellschaft für Nuklearmedizin MedReport 11, 2008.
23 L. S. Yasui, K. Chen, K. Wang, T. P. Jones, J. Caldwell, D. Guse and A. I. Kassis, *Radiation Res*, 2007, **167**, 167–175.
24 P. Balagurumoorthy, K. Wang, J. S. Adelstein and A. I. Kassis, *Int J Radiat Biol*, 2008, **84**, 976–983.
25 O. Dann, G. Bergen, E. Demant and G. Volz, *Liebig Ann Chem*, 1971, **749**, 86–89.
26 A. Krishan and P. D. Dandekar, *J Histochem Cytochem*, 2005, **53**, 1033–1036.
27 A. A. Farahat, A. Kumar, M. Say, F. E. Barghash, Alaa El-Din M. anf Goda, H. M. Eisa, T. Wenzler, R. Brun, Y. Liu, L. Mickelson, D. W. Wilson and D. W. Boykin, *Bioorg Med Chem*, 2010, **18**, 557–566.
28 J. Kapuscinski, *Biochem Histochem*, 1995, **70**, 220–233.
29 C. Zimmer and U. Wähnert, *Prog Biophys molec Biol*, 1986, **47**, 31–112.
30 D. Vlieghe, J. Sponer and L. Van Meervelt, *Biochemistry*, 1999, **38**, 16443–16451.
31 L. F. P. De Castro and M. Zacharias, *J Mol Recognit*, 2002, **15**, 209–220.
32 E. Trotta, E. D'Ambrosio, G. Ravagnan and P. Maurizio, *Nucleic Acids Res*, 1995, **23**, 1333–1340.
33 D. Banerjee and S. K. Pal, *J Phys Chem*, 2008, **112**, 1016–1021.
34 D. A. Schwartz, M. J. Abrams, M. M. Hauser, F. E. Gaul, S. K. Larsen, D. Rauh and J. A. Zubieta, *Bioconj Chem*, 1991, **2**, 333–336.
35 D. J. Rose, K. P. Maresca, T. Nicholson, A. Davison, A. G. Jones, J. Babich, A. Fischman, W. Graham, J. R. D. DeBord and J. Zubieta, *Inorg Chem*, 1998, **37**, 2701–2716.
36 T. D. Harris, M. Sworin, N. Williams, M. Rajopadhye, P. R. Damphousse, D. Glowacka, M. J. Poirier and K. Yu, *Bioconj Chem*, 1999, **10**, 808–814.
37 M.-L. Biechlin, A. Bonmartin, F.-N. Gilly, M. Fraysse and A. du Moulinet d'Hardemare, *Nucl Med Biol*, 2008, **35**, 679–687.
38 M. Bartolomä, J. Valliant, K. P. Maresca, J. Babich and J. Zubieta, *Chem Comm*, 2009, 473–604.
39 L. K. Meszaros, A. Dose, S. C. G. Biagini and P. J. Blower, *Dalton Trans*, 2011, **40**, 6260–6267.
40 M. J. Abrams, M. Juweid, C. I. tenKate, D. A. Schwartz, M. M. Hauser, F. E. Gaul, A. E. Fuccello, R. H. Rubin, H. W. Strauss and A. J. Fischman, *J Nucl Med*, 1990, **31**, 2022–2028.
41 J. W. Babich and A. J. Fischman, *Nucl Med Biol*, 1995, **22**, 25–30.
42 S. R. Banerjee, P. Schaffer, J. W. Babich, J. F. Valliant and J. Zubieta, *Dalton Trans*, 2005, 3886–3897.
43 S. Liu, W.-Y. Hsieh, Y.-S. Kim and S. I. Mohammed, *Bioconj Chem*, 2005, **16**, 1580–1588.
44 M. Li, R. S. Wu and J. S. C. Tsai, *Bioorg Med Chem Lett*, 2003, **13**, 4351–4354.
45 M. Gandomkar, R. Najafi, M. Shafiei and S. E. S. Ebrahimi, *Appl Rad Isotopes*, 2007, **65**, 805–808.
46 M. Bashir-Uddin Surfraz, S. C. G. Biagini and P. J. Blower, *Dalton Trans*, 2008, 2920–2922.
47 M. Bashir-Uddin Surfraz, R. King, S. J. Mather, S. C. G. Biagini and P. J. Blower, *Tetrahedron*, 2010, **66**, 2037–2043.
48 S. Liu and E. S. Harris, *Bioconjug Chem*, 1998, **9**, 583–595.
49 R. C. King, M. Bashir-Uddin Surfraz, P. J. Biagini, Stefano C G abd Blower and S. J. Mather, *Dalton Trans*, 2007, 4998–5007.
50 Z. Darzynkiewicz, F. Traganos, J. Kapuscinski, L. Staiano-Coico and M. R. Melamed, *Cytometry*, 1984, **5**, 355–363.
51 D. J. Bridges, M. K. Gould, B. Nerima, P. Mäser, R. J. S. Burchmore and H. p. de Koning, *Mol Pharmacol*, 2007, **71**, 1098–1108.
52 T. Yasujima, K. Ohta, K. Inoue and H. Yuasa, *J Pharm Sci*, 2011, **100**, 4006–4012.

